Eur. Phys. J. C 25, 103–111 (2002)
Digital Object Identifier (DOI) 10.1007/s10052-002-0972-4

THE EUROPEAN PHYSICAL JOURNAL C

Rare decay $B \to X_s l^+ l^-$ in a CP spontaneously broken two-Higgs doublet model

C.-S. Huang[1], W. Liao[2], Q.-S. Yan[3], S.-H. Zhu[4]

[1] Institute of Theoretical Physics, Academia Sinica, P.O. Box 2735, Beijing 100080, P.R. China
[2] The Abdus Salam International Centre for Theoretical Physics, P.O. Box 586, 34014 Trieste, Italy
[3] Institute of High Energy Physics, Chinese Academy of Sciences, P.O. Box 918-4, Beijing 100039, P.R. China
[4] Institut für Theoretische Physik, Universität Karlsruhe, 76128 Karlsruhe, Germany

Received: 15 October 2001 / Revised version: 5 March 2002 /
Published online: 26 July 2002 –

Abstract. The Higgs boson mass spectrum and couplings of the neutral Higgs bosons to the fermions are worked out in a CP spontaneously broken two-Higgs doublet model in the large $\tan\beta$ case. The differential branching ratio, forward–backward asymmetry, CP asymmetry and lepton polarization for $B \to X_s l^+ l^-$ are computed. It is shown that the effects of neutral Higgs bosons are quite significant when $\tan\beta$ is large. Especially, the CP violating normal polarization $P_{\rm N}$ can be as large as several percents.

1 Introduction

The recent results on CP violation in B_d–$\bar{B}_d$ mixing have been reported by the BaBar and Belle Collaborations [1], which can be explained in the standard model (SM) within theoretical and experimental uncertainties. As is well known, the direct CP violation measurement, $\mathrm{Re}(\epsilon'/\epsilon)$, in the kaon system [2] can also be accommodated by the CKM phase in the SM within the theoretical uncertainties. However, the CKM phase is not enough to explain the matter–antimatter asymmetry in the universe and gives a contribution to electric dipole moments (EDMs) of electron and neutron much smaller than the experimental limits of EDMs of electron and neutron. Therefore, one needs new sources of CP violation, which has been one of the motivations to search new theoretical models beyond the SM.

The minimal extension of the SM is to enlarge the Higgs sector [3]. It has been shown that if one adheres to the natural flavor conservation (NFC) in the Higgs sector, then a minimum of three Higgs doublets are necessary in order to have spontaneous CP violation [4]. However, the constraint can be evaded if one gives up NFC. If NFC is broken, one can obtain a so-called general or model III two-Higgs doublet model (2HDM) in which the CP symmetry is explicitly broken. In this paper, however, we will discuss a simpler 2HDM in which the Higgs potential is CP invariant and Z_2 symmetry softly broken. Comparing with model I or model II 2HDM, the Higgs potential of this model has an additional linear term of $\mathrm{Re}(\phi_1^+\phi_2)$ and different self-couplings for the real and image parts of $\phi_1^+\phi_2$ [5–7]. In this model (we call it model IV 2HDM hereafter) CP symmetry can be spontaneously broken [5–7]. So model IV is minimal among the extensions of the SM that provide a new source of CP violation. It should be noted that, in addition to the above terms, if one adds a linear term of $\mathrm{Im}(\phi_1^+\phi_2)$, then one will obtain a CP softly broken 2HDM [7].

Flavor changing neutral current (FCNC) transitions $B \to X_s\gamma$ and $B \to X_s l^+ l^-$ provide testing grounds for the SM at the loop level and sensitivity to new physics. Rare decays $B \to X_s l^+ l^- (l = e, \mu)$ have been extensively investigated in both SM and beyond [8,9]. In these processes contributions from exchanging neutral Higgs bosons (NHB) can be safely neglected because of the smallness of m_l/m_W $(l = e, \mu)$ if $\tan\beta$ is smaller than about 25. The inclusive decay $B \to X_s\tau^+\tau^-$ has also been investigated in the SM, the model II 2HDM and SUSY models with and without including the contributions of NHB [10–19], in a CP softly broken 2HDM [5], as well as in the technicolor model with scalars [20]. In this paper we investigate $B \to X_s l^+ l^-$ $(l = e, \mu, \tau)$ with emphasis on CP violation effects in model IV. Although there is little difference between the CP softly and spontaneously broken models [7], the mass spectrum and consequently some phenomenological effects are different.

This paper is organized as follows. In Sect. 2, we describe the details of the model IV and work out the Higgs mass spectrum and couplings of Higgs bosons to fermions. Section 3 is devoted to the effective Hamiltonian responsible for $B \to X_s l^+ l^-$. We calculate Wilson coefficients and give all the leading terms. In Sect. 4 the formula for CP violating observables and lepton polarizations in $B \to X_s l^+ l^-$ are given. We give the numerical results in Sect. 5. Finally, in Sect. 6 we draw conclusions and give a discussion.

2 The CP spontaneously broken 2HDM

For two complex $y = 1$, $SU(2)_w$ doublet scalar fields, ϕ_1 and ϕ_2, the simplest Higgs potential, which is NFC softly broken, can be written as [7]

$$\begin{aligned} V(\phi_1, \phi_2) = & \sum_{i=1,2} [m_i^2 \phi_i^+ \phi_i + \lambda_i (\phi_i^+ \phi_i)^2] \\ & + m_3^2 \mathrm{Re}(\phi_1^+ \phi_2) + m_4^2 \mathrm{Im}(\phi_1^+ \phi_2) \\ & + \lambda_3 [(\phi_1^+ \phi_1)(\phi_2^+ \phi_2)] + \lambda_4 [\mathrm{Re}(\phi_1^+ \phi_2)]^2 \\ & + \lambda_5 [\mathrm{Im}(\phi_1^+ \phi_2)]^2. \end{aligned} \tag{1}$$

Hermiticity requires that all parameters are real. It should be noted that the potential is CP softly broken due to the presence of the term $m_4^2 \mathrm{Im}(\phi_1^+ \phi_2)$. We assume that the minimum of the potential is at

$$\langle \phi_1 \rangle = \begin{pmatrix} 0 \\ v_1 \end{pmatrix}, \quad \langle \phi_2 \rangle = \begin{pmatrix} 0 \\ v_2 \mathrm{e}^{\mathrm{i}\xi} \end{pmatrix}, \tag{2}$$

which breaks $SU(2) \times U(1)$ down to $U(1)_{\mathrm{EM}}$ and simultaneously the CP invariance. The requirement that the vacuum is at least a stationary point of the potential results in the following three constraints:

$$\begin{aligned} \sin 2\xi v_1 v_2 (\lambda_4 - \lambda_5) + \sin \xi m_3^2 - \cos \xi m_4^2 = 0, \\ v_2 \cos \xi [2C_2 + v_1^2 (\lambda_4 - \lambda_5)] + v_1 m_3^2 = 0, \\ \sin \xi (v_1^2 C_1 - v_2^2 C_2) - v_1 v_2 m_4^2 = 0, \end{aligned} \tag{3}$$

where

$$\begin{aligned} C_1 &= m_1^2 + 2\lambda_1 v_1^2 + \left(\lambda_3 + \frac{\lambda_4 + \lambda_5}{2} \right) v_2^2, \\ C_2 &= m_2^2 + 2\lambda_2 v_2^2 + \left(\lambda_3 + \frac{\lambda_4 + \lambda_5}{2} \right) v_1^2. \end{aligned} \tag{4}$$

For the CP classically invariant case (model IV), $m_4^2 = 0$, (3) reduces to

$$\begin{aligned} m_1^2 &= -[2\lambda_1 v_1^2 + (\lambda_3 + \lambda_5) v_2^2], \\ m_2^2 &= -[2\lambda_2 v_2^2 + (\lambda_3 + \lambda_5) v_1^2], \\ m_3^2 &= -2 v_1 v_2 (\lambda_4 - \lambda_5) \cos \xi. \end{aligned} \tag{5}$$

From (5), one can see that the necessary condition to have spontaneously broken CP is $\lambda_4 \neq \lambda_5$ and $m_3^2 \neq 0$, i.e., the real and image parts of $\phi_1^+ \phi_2$ have different self-couplings and there exists a linear term of $\mathrm{Re}(\phi_1^+ \phi_2)$ in the potential.

We can write the potential at the stationary point as

$$\begin{aligned} V = & m_1^2 v_1^2 + m_2^2 v_2^2 + \lambda_1 v_1^4 + \lambda_2 v_2^4 + (\lambda_3 + \lambda_5) v_1^2 v_2^2 \\ & + (\lambda_4 - \lambda_5) v_1^2 v_2^2 \left[(\cos \xi - \Delta)^2 - \Delta^2 \right], \end{aligned} \tag{6}$$

with

$$\Delta = -\frac{m_3^2}{2 v_1 v_2 (\lambda_4 - \lambda_5)}.$$

One can see that in order for the spontaneous CP breaking to occur with $\sin \xi \neq 0$, the following inequalities must hold:

$$\lambda_4 - \lambda_5 > 0, \quad -1 < \Delta < 1,$$

and the potential minimum is at $\cos \xi = \Delta$, which is automatically satisfied due to (5).

In the following we will work out the mass spectrum of the Higgs bosons in model IV. For charged components, the mass-squared matrix for negative states is

$$-\lambda_5 \begin{pmatrix} v_1^2 & -v_1 v_2 \mathrm{e}^{\mathrm{i}\xi} \\ -v_1 v_2 \mathrm{e}^{-\mathrm{i}\xi} & v_2^2 \end{pmatrix}. \tag{7}$$

Diagonalizing the mass-squared matrix results in one zero-mass Goldstone state, we have

$$G^- = \mathrm{e}^{\mathrm{i}\xi} \sin \beta \phi_2^- + \cos \beta \phi_1^-, \tag{8}$$

and one massive charged Higgs boson state, we have

$$H^- = \mathrm{e}^{\mathrm{i}\xi} \cos \beta \phi_2^- - \sin \beta \phi_1^-, \tag{9}$$

$$m_{H^-} = |\lambda_5| v^2, \tag{10}$$

where $\tan \beta = v_2 / v_1$ and $v^2 = v_1^2 + v_2^2$, which is determined by $2m_W^2 / g^2$. Correspondingly, we could also get the positive states G^+ and H^+.

For neutral Higgs components, because CP conservation is broken, the mass-squared matrix is 4×4, which can not be simply separated into two 2×2 matrices as usual. After rotating the would-be Goldstone boson $(v_1 \mathrm{Im}\phi_1^0 + v_2 \mathrm{Im}\phi_2^0)/v$ away, the elements of the mass matrix of the three physical neutral Higgs bosons μ_{ij}, in the basis of $\{\mathrm{Re}\phi_1^0, \mathrm{Re}\phi_2^0, (v_2 \mathrm{Im}\phi_1^0 - v_1 \mathrm{Im}\phi_2^0)/v\}$, can be written as

$$\begin{aligned} \mu_{11} &= 4\lambda_1 v_1^2 + (\lambda_4 - \lambda_5) v_2^2 c_\xi^2, \\ \mu_{12} &= v_1 v_2 [2\lambda_3 + \lambda_4 c_\xi^2 + \lambda_5 (1 + s_\xi^2)], \\ \mu_{13} &= \frac{1}{2} (\lambda_4 - \lambda_5) v_2 v s_{2\xi}, \\ \mu_{22} &= 4\lambda_2 v_2^2 + (\lambda_4 - \lambda_5) v_1^2 c_\xi^2, \\ \mu_{23} &= \frac{1}{2} (\lambda_4 - \lambda_5) s_{2\xi} v_1 v, \\ \mu_{33} &= (\lambda_4 - \lambda_5) v^2 s_\xi^2, \end{aligned} \tag{11}$$

where s, c represent $\sin, \cos$. In (11), the constraints in (5) have been used. In the case of large $\tan \beta$ which is what we are interested in[1], if we neglect all terms proportional to v_1, i.e., if the parameters λ_i are of the same order, one can see from the above mass matrix that one of the Higgs boson masses is zero, which is obviously in conflict with current experiments. Therefore, instead we shall discuss the cases in which there is a hierarchy of order of magnitude between the parameters, $\lambda_1 \gg$ the other λ's, and other terms proportional to v_1 in (11) are negligible. For simplicity, we define $\bar{\lambda} = \lambda_4 - \lambda_5$ and $\tilde{\lambda} = 4\lambda_1 v_1^2$. Diagonalizing the Higgs boson mass-squared matrix results in

$$\begin{pmatrix} H_1^0 \\ H_2^0 \\ H_3^0 \end{pmatrix} = \sqrt{2} \begin{pmatrix} c_\alpha & s_\alpha & 0 \\ -s_\alpha & c_\alpha & 0 \\ 0 & 0 & 1 \end{pmatrix} \begin{pmatrix} \mathrm{Im}\phi_1^0 \\ \mathrm{Re}\phi_1^0 \\ \mathrm{Re}\phi_2^0 \end{pmatrix}, \tag{12}$$

[1] In model IV, the fermions obtain masses in the same way as in model II 2HDM. The contributions to the $B \to X_s l^+ l^-$ from exchanging neutral Higgs bosons are enhanced roughly by a factor of $\mathrm{tg}^2 \beta$

with masses

$$m^2_{H^0_1,H^0_2} = \frac{1}{2}\left(\mu_{11}+\mu_{33} \mp \sqrt{(\mu_{11}-\mu_{33})^2+4\mu^2_{13}}\right) \quad (13)$$

and the mixing angle

$$\tan(2\alpha) = \frac{2\mu_{13}}{\mu_{33}-\mu_{11}}. \quad (14)$$

In model IV, it is assumed that the fermions obtain masses in the same way as in model II 2HDM. That is, the up-type quarks get masses from Yukawa couplings to the Higgs doublet ϕ_2 and down-type quarks and leptons get masses from Yukawa couplings to the Higgs doublet ϕ_1. Then it is straightforward to obtain the couplings of neutral Higgs bosons to fermions:

$$\begin{aligned} H^0_1\bar{f}f: &\quad -\frac{\mathrm{i}gm_f}{2m_w c_\beta}(s_\alpha + \mathrm{i}c_\alpha\gamma_5), \\ H^0_2\bar{f}f: &\quad -\frac{\mathrm{i}gm_f}{2m_w c_\beta}(c_\alpha - \mathrm{i}s_\alpha\gamma_5), \end{aligned} \quad (15)$$

where f represents down-type quarks and leptons. The coupling of H^0_3 to f is not enhanced by $\tan\beta$ and will not be given here explicitly. The couplings of the charged Higgs bosons to fermions are the same as those in the CP conservative 2HDM (model II, see [22]). This is in contrast with model III [23] in which the couplings of the charged Higgs to fermions can be quite different from model II. It is easy to see from (15) that the contributions coming from exchanging NHB are proportional to $2^{1/2}G_{\mathrm{F}}s_\alpha c_\alpha m_f^2/\cos^2\beta$, so that the constraint due to EDM translate into the constraint on $\sin 2\alpha \tan^2\beta$ ($1/\cos\beta \sim \tan\beta$ in the large $\tan\beta$ limit). According to the analysis in [24], we have the constraint

$$\sqrt{|\sin 2\alpha|}\tan\beta < 50 \quad (16)$$

from the neutron EDM. And the constraint from the electron EDM is not stronger than (16). It is obvious from (16) that there is a constraint on α only if $\tan\beta > 50$.

3 The effective Hamiltonian for $B \to X_s l^+ l^-$

As is well known, inclusive decay rates of heavy hadrons can be calculated in heavy quark effective theory (HQET) [25] and it has been shown that the leading terms in the $1/m_Q$ expansion turn out to be the decay of a free (heavy) quark and corrections are of the order $1/m_Q^2$ [26]. In what follows we shall calculate the leading term. The effective Hamiltonian describing the flavor changing processes $b \to s l^+ l^-$ can be defined as

$$H_{\mathrm{eff}} = \frac{4G_{\mathrm{F}}}{\sqrt{2}}V_{tb}V^*_{ts}\left(\sum_{i=1}^{10}C_i(\mu)O_i(\mu) + \sum_{i=1}^{10}C_{Q_i}(\mu)Q_i(\mu)\right), \quad (17)$$

where $O_i (i = 1, \cdots, 10)$ is the same as that given in [8]; the Q_i come from exchanging the neutral Higgs bosons and are defined in [12]. The explicit expressions of the operators governing $B \to X_s l^+ l^-$ are given as follows:

$$\begin{aligned} O_7 &= (e/16\pi^2)m_b(\bar{s}_{\mathrm{L}\alpha}\sigma^{\mu\nu}b_{\mathrm{R}\alpha})F_{\mu\nu}, \\ O_8 &= (e/16\pi^2)(\bar{s}_{\mathrm{L}\alpha}\gamma^\mu b_{\mathrm{L}\alpha})\bar{l}\gamma_\mu l, \\ O_9 &= (e/16\pi^2)(\bar{s}_{\mathrm{L}\alpha}\gamma^\mu b_{\mathrm{L}\alpha})\bar{l}\gamma_\mu\gamma_5 l, \\ Q_1 &= (\mathrm{e}^2/16\pi^2)(\bar{s}_{\mathrm{L}\alpha}b_{\mathrm{R}\alpha})(\bar{l}l), \\ Q_2 &= (\mathrm{e}^2/16\pi^2)(\bar{s}_{\mathrm{L}\alpha}b_{\mathrm{R}\alpha})(\bar{l}\gamma_5 l). \end{aligned} \quad (18)$$

For the large $\tan\beta$ case, we can generally write the couplings as follows:

$$\begin{aligned} HH^\pm G^\mp: &\quad \pm\mathrm{i}gC_{HH^+G^-}, \\ HH^\pm W^\mp: &\quad \mathrm{i}gC_{HH^+W^-}, \\ H\bar{b}b: &\quad \mathrm{i}gm_b\tan\beta(C_b + \bar{C}_b\gamma_5), \\ H\bar{l}l: &\quad \mathrm{i}gm_l\tan\beta(C_l + \bar{C}_l\gamma_5). \end{aligned} \quad (19)$$

In model VI, we obtain

$$\begin{aligned} C_{H_1H^+G^-} &= -\sqrt{2}v\mathrm{e}^{\mathrm{i}\xi} \\ &\quad \times\left[c_\alpha(\lambda_4 s_\xi + \mathrm{i}\lambda_5 c_\xi) + s_\alpha(\lambda_4 c_\xi - \mathrm{i}\lambda_5 s_\xi + \tilde{\lambda})\right], \\ C_{H_2H^+G^-} &= -\sqrt{2}v\mathrm{e}^{\mathrm{i}\xi}\Big[-s_\alpha(\lambda_4 s_\xi + \mathrm{i}\lambda_5 c_\xi) \\ &\quad + c_\alpha(\lambda_4 c_\xi - \mathrm{i}\lambda_5 s_\xi + \tilde{\lambda})\Big], \\ C_{H_1H^+W^-} &= -\frac{s_\alpha + \mathrm{i}c_\alpha}{2}, \\ C_{H_2H^+W^-} &= -\frac{c_\alpha - \mathrm{i}s_\alpha}{2}. \end{aligned} \quad (20)$$

and $C_b, C_l, \bar{C}_b, \bar{C}_l$ can be extracted from (15).

At the renormalization point $\mu = m_W$ the coefficients C_i in the effective Hamiltonian have been given in [8] and the C_{Q_i} are (neglecting the $O(\mathrm{tg}\beta)$ term)

$$\begin{aligned} C_{Q_1}(m_W) &= \frac{m_b m_l \mathrm{tg}^2\beta x_t}{\sin^2\theta_W}\left\{\frac{1}{m_H^2}\left[-m_W^2(C_b+\bar{C}_b)f_1\right.\right. \\ &\quad \left.\left. + C_{HH^+G^-}f_2 - m_W C_{HH^+W^-}f_2\right]C_l - \frac{f_3}{4m_W^2}\right\}, \\ C_{Q_2}(m_W) &= \frac{m_b m_l \mathrm{tg}^2\beta x_t}{\sin^2\theta_W}\left\{\frac{1}{m_H^2}\left[-m_W^2(C_b+\bar{C}_b)f_1\right.\right. \\ &\quad \left.\left. + C_{HH^+G^-}f_2 - m_W C_{HH^+W^-}f_2\right]\bar{C}_l + \frac{f_3}{4m_W^2}\right\}, \\ C_{Q_3}(m_W) &= \frac{m_b e^2}{m_l g_s^2}(C_{Q_1}(m_W) + C_{Q_2}(m_W)), \\ C_{Q_4}(m_W) &= \frac{m_b e^2}{m_l g_s^2}(C_{Q_1}(m_W) - C_{Q_2}(m_W)), \\ C_{Q_i}(m_W) &= 0, \quad i = 5, \cdots, 10, \end{aligned} \quad (21)$$

where

$$\begin{aligned} f_1 &= \frac{x_t\ln x_t}{x_t-1} - \frac{x_{H^\pm}\ln x_{H^\pm} - x_t\ln x_t}{x_{H^\pm}-x_t}, \\ f_2 &= \frac{x_t\ln x_t}{(x_t-1)(x_{H^\pm}-x_t)} - \frac{x_{H^\pm}\ln x_{H^\pm}}{(x_{H^\pm}-x_t)(x_{H^\pm}-1)}, \\ f_3 &= \frac{1}{x_{H^\pm}-x_t}\left(\frac{\ln x_t}{x_t-1} - \frac{\ln x_{H^\pm}}{x_{H^\pm}-1}\right), \end{aligned} \quad (22)$$

with $x_i = m_i^2/m_w^2$. It would be instructive to note that in addition to the diagrams of exchanging neutral Higgs bosons, the box diagram with a charged Higgs and a W in the loop also gives a leading contribution proportional to $\tan^2\beta$ [27,28].

Neglecting the strange quark mass, the effective Hamiltonian (17) leads to the following matrix element for $b \to s l^+ l^-$:

$$M = \frac{G_{\rm F}\alpha}{\sqrt{2}\pi} V_{tb}V_{ts}^* \Bigg[C_8^{\rm eff}\bar{s}_{\rm L}\gamma_\mu b_{\rm L}\bar{l}\gamma^\mu l + C_9 \bar{s}_{\rm L}\gamma_\mu b_{\rm L}\bar{l}\gamma^\mu\gamma^5 l + 2C_7 m_b \bar{s}_{\rm L}{\rm i}\sigma^{\mu\nu}\frac{q^\nu}{q^2} b_{\rm R}\bar{l}\gamma^\mu l + C_{Q_1}\bar{s}_{\rm L}b_{\rm R}\bar{l}l + C_{Q_2}\bar{s}_{\rm L}b_{\rm R}\bar{l}\gamma^5 l \Bigg], \quad (23)$$

where [8,10,29]

$$C_8^{\rm eff} = C_8 + \left\{ g\left(\frac{m_c}{m_b}, \hat{s}\right) + \frac{3}{\alpha^2}k \sum_{V_i = J/\psi, \psi', \psi''\ldots} \times \frac{\pi M_{V_i}\Gamma(V_i \to l^+l^-)}{M_{V_i}^2 - q^2 - {\rm i}M_{V_i}\Gamma_{V_i}} \right\} (3C_1 + C_2), \quad (24)$$

with $\hat{s} = q^2/m_b^2$, $q = (p_{\mu^+} + p_{\mu^-})^2$. In (24) $g\,(m_c/m_b, \hat{s})$ arises from the one-loop matrix element of the four-quark operators and can be found in [8,30]. The second term in the braces in (24) estimates the long-distance contribution from the intermediates, J/ψ, ψ', ψ''... [8,29]. For $l = \tau$, the lowest resonance J/ψ in the $c\bar{c}$ system does not contribute because the invariant mass square of the lepton pair is $s > 4m_\tau^2$. In our numerical calculations, we choose $k(3C_1 + C_2) = -0.875$ [31].

The QCD corrections to coefficients C_i and C_{Q_i} can be incorporated in the standard way by using the renormalization group equations. Although the C_i at the scale $\mu = O(m_b)$ have been given in the next-to-leading order approximation (NLO) without including mixing with Q_i [32], we use the values of C_i only in the leading order approximation (LO) since no C_{Q_i} have been calculated in NLO. The C_i and C_{Q_i} with LO QCD corrections at the scale $\mu = O(m_b)$ have been given in [12]:

$$C_7(m_b) = \eta^{-16/23}\left[C_7(m_W) - \left[\frac{58}{135}(\eta^{10/23} - 1) + \frac{29}{189}(\eta^{28/23} - 1)\right] C_2(m_W) - 0.012 C_{Q_3}(m_W)\right], \quad (25)$$

$$C_8(m_b) = C_8(m_W) + \frac{4\pi}{\alpha_{\rm s}(m_W)} \times \left[-\frac{4}{33}(1 - \eta^{-11/23}) + \frac{8}{87}(1 - \eta^{-29/23})\right] C_2(m_W), \quad (26)$$

$$C_9(m_b) = C_9(m_W), \quad (27)$$

$$C_{Q_i}(m_b) = \eta^{-\gamma_Q/\beta_0} C_{Q_i}(m_W), \quad i = 1, 2, \quad (28)$$

where $\gamma_Q = -4$ [33] is the anomalous dimension of $\bar{s}_{\rm L} b_{\rm R}$, $\beta_0 = 11 - 2n_f/3$, and $\eta = \alpha_{\rm s}(m_b)/\alpha_{\rm s}(m_W)$.

After a straightforward calculation, we obtain the invariant dilepton mass distribution [12]

$$\begin{aligned} &\frac{{\rm d}\Gamma(B \to X_s l^+ l^-)}{{\rm d}s} \\ &= B(B \to X_c l\bar{\nu})\frac{\alpha^2}{4\pi^2 f(m_c/m_b)}(1 - s)^2 \\ &\times \left(1 - \frac{4t^2}{s}\right)^{1/2} \frac{|V_{tb}V_{ts}^*|^2}{|V_{cb}|^2} D(s) \\ &D(s) = |C_8^{\rm eff}|^2\left(1 + \frac{2t^2}{s}\right)(1 + 2s) \\ &+ 4|C_7|^2\left(1 + \frac{2t^2}{s}\right)\left(1 + \frac{2}{s}\right) \\ &+ |C_9|^2\left[(1 + 2s) + \frac{2t^2}{s}(1 - 4s)\right] \\ &+ 12{\rm Re}(C_7 C_8^{\rm eff*})\left(1 + \frac{2t^2}{s}\right) \\ &+ \frac{3}{2}|C_{Q_1}|^2(s - 4t^2) + \frac{3}{2}|C_{Q_2}|^2 s + 6{\rm Re}(C_9 C_{Q_2}^*)t, \end{aligned} \quad (29)$$

where $s = q^2/m_b^2$, $t = m_l/m_b$, $B(B \to X_c l\bar{\nu})$ is the branching ratio of $B \to X_c l\bar{\nu}$, f is the phase-space factor and $f(x) = 1 - 8x^2 + 8x^6 - x^8 - 24x^4\ln x$.

We also give the forward–backward asymmetry

$$\begin{aligned} A(s) &= \frac{\displaystyle\int_0^1 {\rm d}z \frac{{\rm d}^2\Gamma}{{\rm d}s{\rm d}z} - \int_{-1}^0 {\rm d}z \frac{{\rm d}^2\Gamma}{{\rm d}s{\rm d}z}}{\displaystyle\int_0^1 {\rm d}z \frac{{\rm d}^2\Gamma}{{\rm d}s{\rm d}z} + \int_{-1}^0 {\rm d}z \frac{{\rm d}^2\Gamma}{{\rm d}s{\rm d}z}} \\ &= -3\sqrt{\frac{1 - 4t^2}{s}}\frac{E(s)}{D(s)}, \end{aligned} \quad (30)$$

where $z = \cos\theta$ and θ is the angle between the momentum of the B-meson and that of l^+ in the center of mass frame of the dileptons l^+l^-. Here,

$$E(s) = {\rm Re}(C_8^{\rm eff} C_9^* s + 2C_7 C_9^* + C_8^{\rm eff} C_{Q1}^* t + 2C_7 C_{Q2}^* t). \quad (31)$$

4 CP-violating observables and lepton polarizations in $B \to X_s l^+ l^-$

The formulas for CP violating observables and lepton polarizations in $B \to X_s l^+ l^-$ have been given in our previous paper [5]. We give the formula below in order to make the present paper self-contained. The CP asymmetry for the $B \to X_s l^+ l^-$ and $\overline{B} \to \overline{X}_s l^+ l^-$ is commonly defined as

$$A_{CP}(s) = \frac{{\rm d}\Gamma/{\rm d}s - {\rm d}\overline{\Gamma}/{\rm d}s}{{\rm d}\Gamma/{\rm d}s + {\rm d}\overline{\Gamma}/{\rm d}s}. \quad (32)$$

The CP asymmetry in the forward–backward asymmetry for $B \to X_s l^+ l^-$ and $\overline{B} \to \overline{X}_s l^+ l^-$ is defined as

$$B_{CP}(s) = A(s) - \overline{A}(s). \quad (33)$$

It is easy to see from (29) that the CP asymmetry A_{CP}, in general, is very small because the weak phase difference in $C_7 C_8^{\rm eff}$ arises from the small mixing of O_7 with Q_3 (see (25)). In contrast to A_{CP}, B_{CP} can reach a large value when $\tan\beta$ is large, as can be seen from (31) and (21). Therefore, we propose to measure B_{CP} in order to search for new CP violation sources.

Let us now discuss the lepton polarization effects. We define three orthogonal unit vectors:

$$\vec{e}_{\rm L} = \frac{\vec{p}_1}{|\vec{p}_1|},$$
$$\vec{e}_{\rm N} = \frac{\vec{p}_s \times \vec{p}_1}{|\vec{p}_s \times \vec{p}_1|},$$
$$\vec{e}_{\rm T} = \vec{e}_{\rm N} \times \vec{e}_{\rm L},$$

where $\vec{p}_1$ and $\vec{p}_s$ are the three momenta of the ℓ^- lepton and the s quark, respectively, in the center of mass of the $\ell^+\ell^-$ system. The differential decay rate for any given spin direction $\vec{n}$ of the ℓ^- lepton, where $\vec{n}$ is a unit vector in the ℓ^- lepton rest frame, can be written as

$$\frac{{\rm d}\Gamma(\vec{n})}{{\rm d}s} = \frac{1}{2}\left(\frac{{\rm d}\Gamma}{{\rm d}s}\right)_0 \left[1 + (P_{\rm L}\vec{e}_{\rm L} + P_{\rm N}\vec{e}_{\rm N} + P_{\rm T}\vec{e}_{\rm T})\cdot\vec{n}\right], \tag{34}$$

where the subscript "0" corresponds to the unpolarized case, and $P_{\rm L}, P_{\rm T}$, and $P_{\rm N}$, which correspond to the longitudinal, transverse and normal projections of the lepton spin, respectively, are functions of s. From (34), one has

$$P_i(s) = \frac{\frac{{\rm d}\Gamma}{{\rm d}s}(\vec{n}=\vec{e}_i) - \frac{{\rm d}\Gamma}{{\rm d}s}(\vec{n}=-\vec{e}_i)}{\frac{{\rm d}\Gamma}{{\rm d}s}(\vec{n}=\vec{e}_i) + \frac{{\rm d}\Gamma}{{\rm d}s}(\vec{n}=-\vec{e}_i)}. \tag{35}$$

The calculations for the P_i (i = L, T, N) lead to the following results:

$$P_{\rm L} = \left(1 - \frac{4t^2}{s}\right)^{1/2} \frac{D_{\rm L}(s)}{D(s)},$$
$$P_{\rm N} = \frac{3\pi}{4s^{1/2}}\left(1 - \frac{4t^2}{s}\right)^{1/2} \frac{D_{\rm N}(s)}{D(s)},$$
$$P_{\rm T} = -\frac{3\pi t}{2s^{1/2}}\frac{D_{\rm T}(s)}{D(s)}, \tag{36}$$

where

$$D_{\rm L}(s) = {\rm Re}\left(2(1+2s)C_8^{\rm eff}C_9^* + 12C_7C_9^* - 6tC_{Q_1}C_9^* - 3sC_{Q_1}C_{Q_2}^*\right),$$
$$D_{\rm N}(s) = {\rm Im}\left(2sC_{Q_1}C_7^* + sC_{Q_1}C_8^{\rm eff*} + sC_{Q_2}C_9^* + 4tC_9C_7^* + 2tsC_8^{\rm eff*}C_9\right),$$
$$D_{\rm T}(s) = {\rm Re}\Bigg(-2C_7C_9^* + 4C_8^{\rm eff}C_7^* + \frac{4}{s}|C_7|^2 - C_8^{\rm eff}C_9^* + s|C_8^{\rm eff}|^2 - \frac{s-4t^2}{2t}C_{Q_1}C_9^* - \frac{s}{t}C_{Q_2}C_7^* - \frac{s}{2t}C_8^{\rm eff}C_{Q_2}^*\Bigg). \tag{37}$$

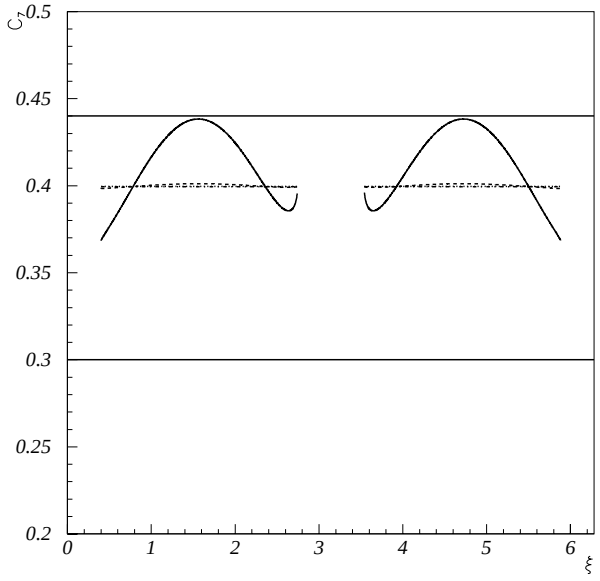

Fig. 1. C_7 as a function of ξ with $m_{H^\pm} = 250GeV$, and *solid* and *dashed lines* represent $\tan\beta = 50$ and 10, *dot-dashed line* represents the case of switching off C_{Q_i} contributions. The region between two straight solid lines is permitted by the $b \to s\gamma$ experiment

P_i (i = L, T, N) have been given in [15], where there are some errors in $P_{\rm T}$ and these authors gave only two terms in $D_{\rm N}$, the numerator of $P_{\rm N}$. We recall that $P_{\rm N}$ is the CP violating projection of the lepton spin onto the normal of the decay plane. Because $P_{\rm N}$ in $B \to X_s l^+ l^-$ comes from both the quark and lepton sectors, purely hadronic and leptonic CP violating observables, such as d_n or d_e, do not necessarily strongly constrain $P_{\rm N}$ [34]. So it is advantageous to use $P_{\rm N}$ to investigate CP violation effects in some extensions of SM [35]. In model IV, as pointed out above, d_n and d_e constrain $(|\sin 2\alpha|)^{1/2}\tan\beta$ and consequently $P_{\rm N}$ through C_{Q_i} ($i = 1, 2$) (see (37)).

5 Numerical results

The following parameters have been used in the numerical calculations:

$$m_{t,\rm pole} = 175\,{\rm GeV}, \quad m_{b,\rm pole} = 5.0\,{\rm GeV},$$
$$m_{c,\rm pole} = 1.3\,{\rm GeV},$$
$$m_\mu = 0.105\,{\rm GeV}, \quad m_\tau = 1.777\,{\rm GeV}, \quad \eta = 1.67.$$

Without losing generality, we assume $0 < \xi < 2\pi$. For the Higgs masses, as an example, we choose $m_{H^\pm} = 250\,{\rm GeV}$ (see discussions below), the lightest neutral Higgs mass being fixed to 100 GeV, and the heavier neutral Higgs mass being 500 GeV. It should be pointed out that the region of ξ will be constrained due to this specific choice of neutral Higgs boson masses (see (13)), which is the reason why there are gaps in Fig. 1 and Figs. 4–10. For $l = e$, the contributions of the neutral Higgs bosons are negligible due to the smallness of the electron mass so that the

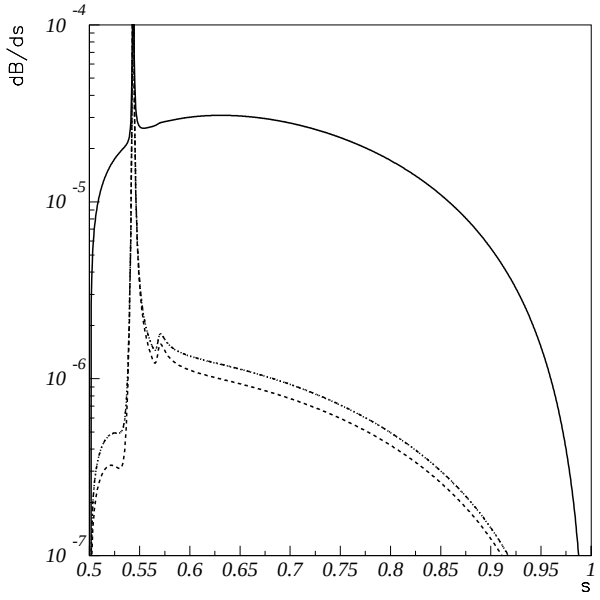

Fig. 2. Differential branching ratio as function of s for $B \to X_s\tau^+\tau^-$, where $\xi = \pi/3$, *solid* and *dashed lines* represent $\tan\beta = 50$ and 10, *dot-dashed line* represents the case of switching off C_{Q_i} contributions

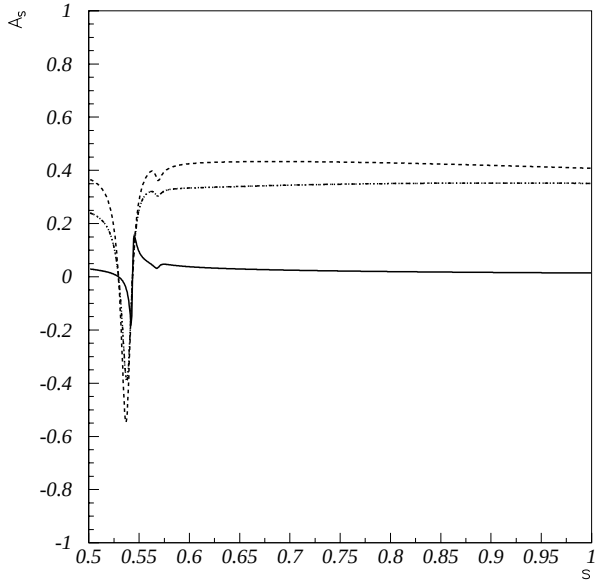

Fig. 3. Forward-backward asymmetry as function of s, other captions are same as Fig. 2

results are almost the same as those in SM. So we only give numerical results for $l = \mu, \tau$. We shall analyze the constraint from $b \to s\gamma$ in the first subsection and give the numerical results for $l = \tau, \mu$ in the second and third subsections respectively.

5.1 The constraint from $b \to s\gamma$

Because the couplings of the charged Higgs to fermions in model IV are the same as those in model II, the constraint on $\tan\beta$ due to effects arising from the charged Higgs are the same as those in the model II. The constraint on $\mathrm{tg}\beta$ from K–$\bar{K}$ and B–$\bar{B}$ mixing, $\Gamma(b \to s\gamma)$, $\Gamma(b \to c\tau\bar{\nu}_\tau)$ and R_b has been given in [36]:

$$0.7 \leq \mathrm{tg}\beta \leq 0.52 \left(\frac{m_{H^\pm}}{1\,\mathrm{GeV}}\right) \tag{38}$$

(and the lower limit $m_{H^\pm} \geq 200\,\mathrm{GeV}$ has also been given in [36]). In [37], it is pointed out that the lower bound of the charged Higgs is about 250 GeV if one adopts a conservative approach to evaluate the theoretical uncertainty; on the other hand, adding different theoretical errors in quadrature leads to $m_{H^\pm} > 370\,\mathrm{GeV}$. Indeed, these bounds are quite sensitive to the errors of the theoretical predictions and to the details of the calculations.

Due to the mixing of O_7 with Q_3, $C_7(\mu)$ is dependent of C_{Q_3} (see (37)). So we have to see if the experimental results of $b \to s\gamma$ impose a constraint on our model parameters (see [38] for a detailed discussion of the constraint on C_7). From the equation [39,40]

$$\frac{B(B \to X_s\gamma)}{B(B \to X_c e\bar{\nu}_e)} = \frac{|V_{ts}^* V_{tb}|^2}{|V_{cb}|^2} \frac{6\alpha}{\pi f(z)} |C_7^{\mathrm{eff}}(\mu_b)|^2 \tag{39}$$

and the experimental results for $b \to s\gamma$ [41]

$$2.0 \times 10^{-4} < B(b \to s\gamma) < 4.5 \times 10^{-4}, \tag{40}$$

we can get the constraint on $|C_7|$. In Fig. 1, we show the C_7 as a function of ξ. One can see from the figure that even for $\tan\beta = 50$, the model can still escape the experimental constraint.

5.2 $B \to X_s\tau^+\tau^-$

Numerical results for $B \to X_s\tau^+\tau^-$ are shown in Figs. 2–7. From Figs. 2 and 3, we can see that the contributions of the NHBs to the differential branching ratio $\mathrm{d}\Gamma/\mathrm{d}s$ and forward–backward asymmetry A_s are significant when $\tan\beta$ is 50 and the masses of NHBs are in a reasonable region, which is similar to the case of model II 2HDM without CP violation [12].

Figures 4 and 5 are devoted to B_{CP} and P_{N} as a function of ξ. From Fig. 4, one can see that B_{CP} can reach about 1.5% for the favorable parameters, and depends strongly on ξ. Figure 5 shows that P_{N} depends also strongly on ξ and can be as large as 8%. It should be noted that experimentally the observables after integrating s are more accessible than those for specific s; therefore we present also the integrated P_{N} (the integration range of s is 0.6–1 which is apart from the resonance region) in Figs. 5 and 8. Our numerical results (Fig. 5b) show that the shape of the integrated P_{N}, which can also reach several percent, is similar to that for specific s. For illumination purposes, we shall present the results for specific s in most of the figures.

Figures 6 and 7 show the longitudinal and transverse polarizations respectively. It is obvious that the contributions of the NHBs can change the polarizations greatly,

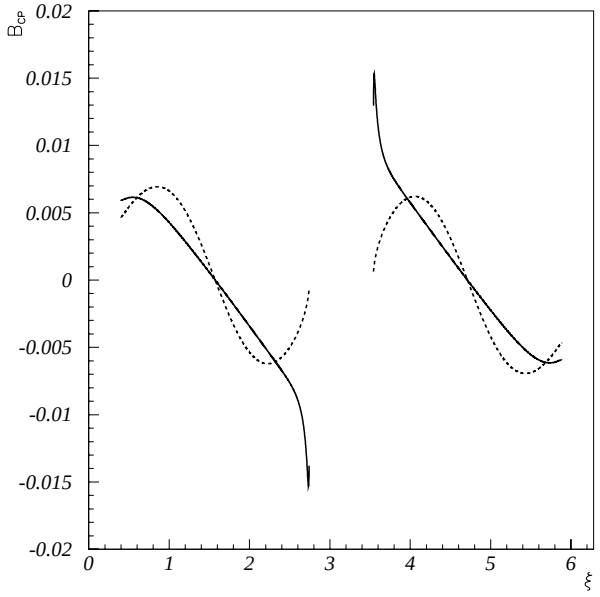

Fig. 4. B_{CP} as function of ξ, for $B \to X_s\tau^+\tau^-$, where $s = 0.8$, solid and dashed lines represent $\tan\beta = 50$ and 10

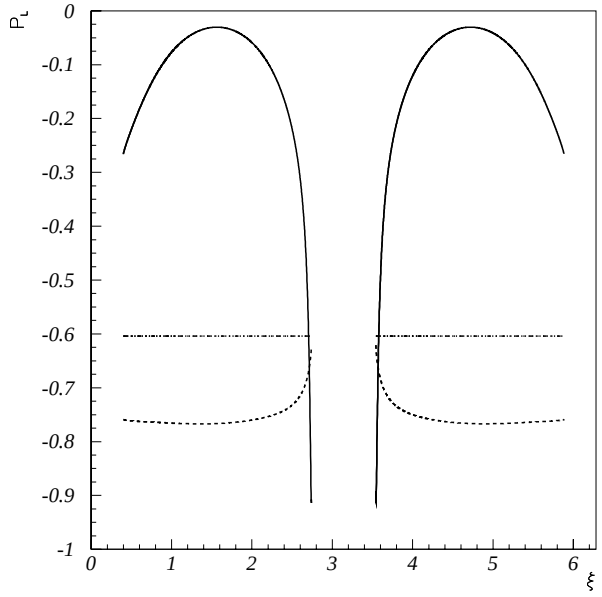

Fig. 6. P_L as function of ξ, other captions are same as Fig. 5a

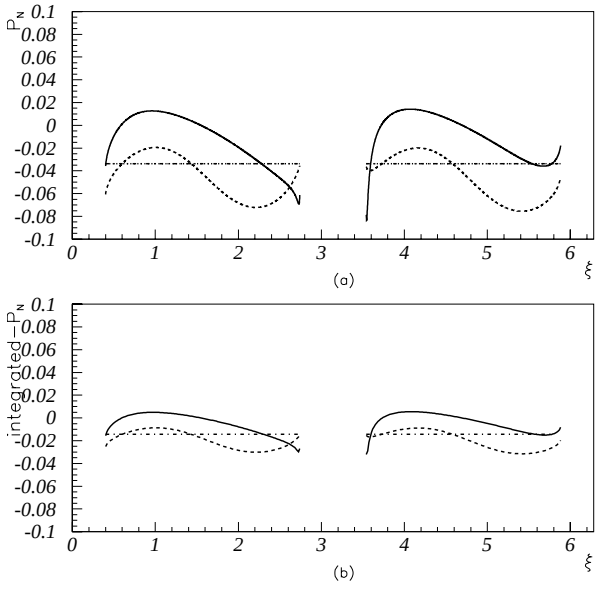

Fig. 5a,b. P_N **a** and integrated-P_N **b** as functions of ξ for $B \to X_s\tau^+\tau^-$, where $s = 0.8$ for **a**, *solid* and *dashed lines* represent $\tan\beta = 50$ and 10, *dot-dashed line* represents the case of switching off C_{Q_i} contributions

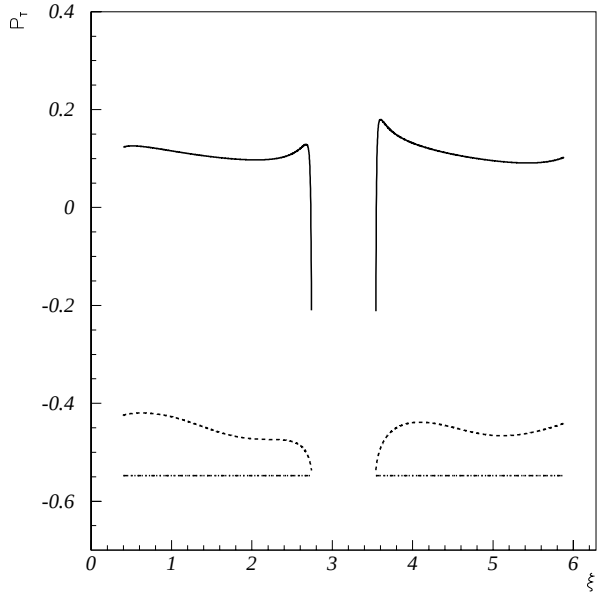

Fig. 7. P_T as function of ξ, other captions are same as Fig. 5a

especially when $\tan\beta$ is large. The longitudinal polarization of $B \to X_s l^+ l^-$ has been calculated in SM and several new physics scenarios [10]. Switching off the NHB contributions, our results are in agreement with those in [10].

5.3 $B \to X_s\mu^+\mu^-$

Because the contributions of the NHBs to the differential branching ratio, forward–backward asymmetry and B_{CP} for the process $B \to X_s\mu^+\mu^-$ are so small if even $\tan\beta$ is as large as 100, which is due to the strong suppression ($\propto m_l^2/m_w^2$), that we do not show the results here. However, for the lepton polarizations, the suppression is proportional to m_l/m_w, which is not so strong, and consequently the NHBs can make relatively significant contributions. We show the numerical result of $P_{\rm N}$ and integrated $P_{\rm N}$ in Fig. 8, and $P_{\rm L}$ and $P_{\rm T}$ in Figs. 9 and 10.

Figure 8 shows that $P_{\rm N}$ is sensitive to ξ and can reach several percent when $\tan\beta = 50$. For $\tan\beta = 10$, $P_{\rm N}$ is unobservably small. From Figs. 9 and 10, one can see that the contributions of the NHBs can change the longitudinal and transverse polarizations greatly, especially when $\tan\beta$ is large.

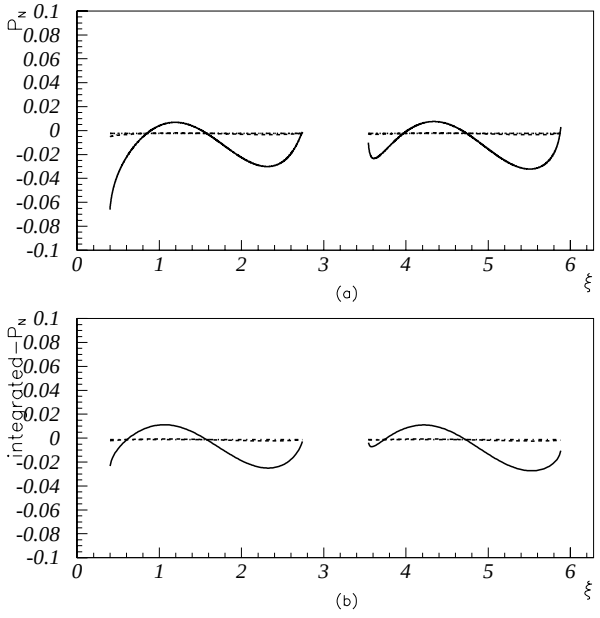

Fig. 8a,b. P_N **a** and integrated-P_N **b** as functions of ξ for $B \to X_s \mu^+ \mu^-$, where $s = 0.6$ for (a), *solid* and *dashed lines* represent $\tan\beta = 50$ and 10, *dot-dashed line* represents the case of switching off C_{Q_i} contributions

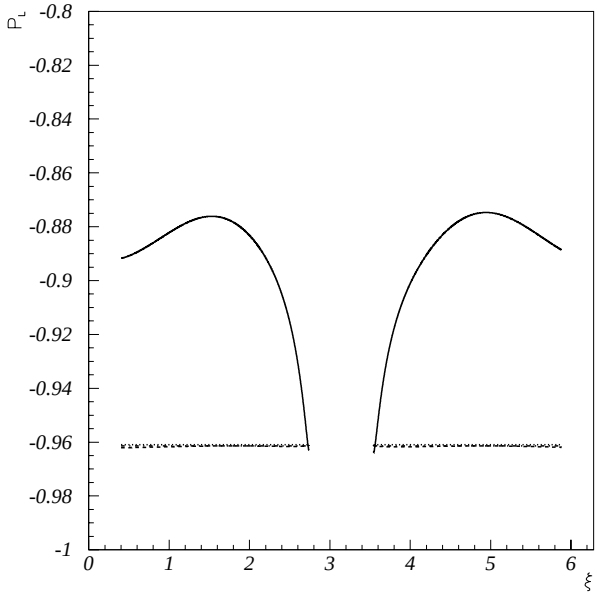

Fig. 9. P_L as function of ξ, other captions are same as Fig. 8a

6 Conclusions and discussions

In summary, we have calculated the differential branching ratio, backward–forward asymmetry, lepton polarizations and some CP violated observables for $B \to X_s l^+ l^-$ in model IV 2HDM. As main features of the model, the NHBs play an important role in inducing CP violation, in particular, for large $\tan\beta$. We propose to measure B_{CP} (defined in Sect. 4) instead of the usual CP asymmetry A_{CP}, because the former could be observed for $l = \tau$ if $\tan\beta$ is large enough and the latter is too small to be

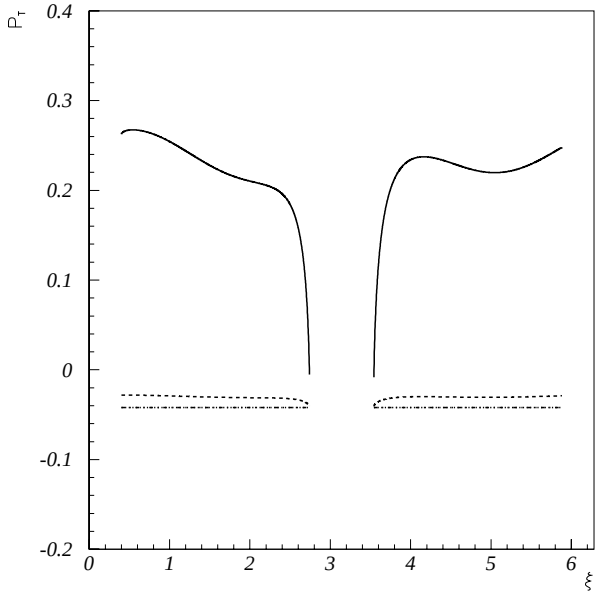

Fig. 10. P_T as function of ξ, other captions are same as Fig. 8a

observed. The CP violating normal polarization $P_{\rm N}$ can reach several percent for $l = \tau$ and μ when $\tan\beta$ is large and Higgs boson masses are in a reasonable range, which could be observed in future B factories with 10^8–10^{12} B hadrons per year [42]. It should be noted that the results are sensitive to the mass of the charged Higgs boson. If the charged Higgs boson is heavy (say $> 400\,\text{GeV}$), the effects arising from new physics would disappear. If we take the mass of the charged Higgs boson to be 200 GeV, which is the lowest limit allowed by $B \to X_s\gamma$, the CP violation effects will be more significant than those given in the paper. Comparing the results in this paper with those in the CP softly broken 2HDM, the main difference is the different ξ-dependence. Therefore, it is possible to discriminate model IV from the other 2HDMs by measuring the CP violated observables such as B_{CP}, $P_{\rm N}$ if nature chooses a large $\tan\beta$ and a light charged Higgs boson. Otherwise, it is difficult to discriminate them.

Acknowledgements. This research was supported in part by the National Nature Science Foundation of China and the Alexander von Humboldt Foundation.

References

1. D. Hitlin (BaBar Collaboration), H. Aihara (Belle Collaboration), in Proceedings (ICHEP2000) edited by C.S. Lim, T. Yamanaka (Singapore, World Scientific 2001)
2. A. Alavi-Harati et al., Phys. Rev. Lett. **83**, 22 (1999); G.D. Barr et al. (NA31 Collaboration), Phys. Lett. B **317**, 233 (1993); V. Fanti et al. (NA48 Collaboration), Phys. Lett. B **465**, 335 (1999) [hep-ex/9909022]
3. T.D. Lee, Phys. Rev. D **8**, 1226 (1973); Phys. Rep. **9c**, 143 (1974); P. Sikivie, Phys. Lett. B **65**, 141 (1976)
4. S. Weinberg, Phys. Rev. Lett. **37**, 657 (1976); G.C. Branco, Phys. Rev. D **22**, 2901 (1980); K. Shizuya, S.-H.H. Tye, Phys. Rev. D **23**, 1613 (1981)

5. Chao-Shang Huang, Shou Hua Zhu, Phys. Rev. D **61**, 015011 (2000); E: D **61**, 119903 (2000)
6. I. Vendramin, hep-ph/9909291
7. H. Georgi, Hadronic J. **1**, 155 (1978)
8. B. Grinstein, M.J. Savage, M.B. Wise, Nucl. Phys. B **319**, 271 (1989)
9. C.S. Huang, W. Liao, Q.S. Yan, Phys. Rev. D **59**, 011701 (1999); T. Goto, Y.Y. Keum, T. Nihei, Y. Okada, Y. Shimizu, Phys. Lett. B **460**, 333 (1999) [hep-ph/9812369]; S. Baek, P. Ko, Phys. Lett. B **462**, 95 (1999) [hep-ph/9904283]; Y.G. Kim, P. Ko, J.S. Lee, Nucl. Phys. B **544**, 64 (1999); C.W. Bauer, C.N. Burrell, Phys. Rev. D **62**, 114028 (2000); E. Gabriclli, S. Khalil, hep-ph/0201049. For the earlier references, see, for example, the references in [12] and [17]
10. J.L. Hewett, Phys. Rev. D **53**, 4964 (1996)
11. Y. Grossman, Z. Ligeti, E. Nardi, Phys. Rev. D **55**, 2768 (1997)
12. Y.B. Dai, C.S. Huang, H.W. Huang, Phys. Lett. B **390**, 257 (1997), E: B **513**, (2001); C.S. Huang, Q.S. Yan, Phys. Lett. B **442**, 209 (1998)
13. S. Fukae, C.S. Kim, T. Yoshikawa, Phys. Rev. D **61**, 074015 (2000) [hep-ph/9908229]
14. F. Krüger, L.M. Sehgal, Phys. Lett. B **380**, 199 (1996)
15. S. Rai Choudhury, A. Gupta, N. Gaur, Phys. Rev. D **60**, 115004 (1999) [hep-ph/9902355]
16. E. Lunghi, I. Scimemi, Nucl. Phys. B **574**, 43 (2000) [hep-ph/9912430]
17. C.-S. Huang, Nucl. Phys. B (Proc. Suppl.) **93**, 73 (2001) and references therein
18. C. Bobeth, T. Ewerth, F. Kruger, J. Urban, Phys. Rev. D **64**, 074014 (2001) [hep-ph/0104284]
19. Z.h. Xiong, J.M. Yang, hep-ph/0105260; E.O. Iltan, G. Turan, Phys. Rev. D **63**, 115007 (2001)
20. Z.h. Xiong, J.M. Yang, Nucl. Phys. B **602**, 289 (2001) [hep-ph/0012217]
21. A. Ali, G. Hiller, Eur. Phys. J. C **8**, 619 (1999); F. Kruger, L.M. Sehgal, Phys. Rev. D **55**, 2799 (1997)
22. J.F. Gunion, H.E. Haber, G. Kane, S. Dawson, The Higgs hunter's guide (Addison-Wesley, MA 1990)
23. See, for example, Y.L. Wu, L. Woffenstein, Phys. Rev. Lett. **73**, 1762 (1994); D. Bowser-Chao, K. Cheung, W.Y. Keung, Phys. Rev. D **59**, 115006 (1999) [hep-ph/9811235], and references therein
24. N.G. Deshpande, E. Ma, Phys. Rev. D **16**, 1583 (1977); A.A. Anselm et al., Phys. Lett. B **152**, 116 (1985); T.P. Cheng, L.F. Li, Phys. Lett. B **234**, 165 (1990); S. Weinberg, Phys. Rev. Lett. **63**, 2333 (1989); X.-G. He, B.H.J. McKellar, Phys. Rev. D **42**, 3221 (1990); E: D **50**, 4719 (1994)
25. For a comprehensive review, see: M. Neubert, Phys. Rep. **245**, 396 (1994)
26. I.I. Bigi, M. Shifman, N.G. Vraltsev, A.I. Vainshtein, Phys. Rev. Lett. **71**, 496 (1993); B. Blok, L. Kozrakh, M. Shifman, A.I. Vainshtein, Phys. Rev. D **49**, 3356 (1994); A.V. Manohar, M.B. Wise, Phys. Rev. D **49**, 1310 (1994); S. Balk, T.G. Körner, D. Pirjol, K. Schilcher, Z. Phys. C **64**, 37 (1994); A.F. Falk, Z. Ligeti, M. Neubert, Y. Nir, Phys. Lett. B **326**, 145 (1994)
27. H.E. Logan, U. Nierste, Nucl. Phys. B **586**, 39 (2000) [hep-ph/0004139]
28. C.-S. Huang, W. Liao, Q.-S. Yan, S.-H. Zhu, Phys. Rev. D **63**, 114021 (2001); E: D **64**, 059902 (2001)
29. N.G. Deshpande, J. Trampetic, K. Ponose, Phys. Lett. B **214**, 467 (1988); Phys. Rev. D **39**, 1461 (1989); C.S. Lim, T. Morozumi, A.I. Sanda, Phys. Lett. B **218**, 343 (1989); A. Ali, T. Mannel, T. Morozumi, Phys. Lett. B **273**, 505 (1991); P.J. O'Donnell, H.K. Tung, Phys. Rev. D **43**, R2067 (1991); G. Buchalla, A. Buras, M. Lautenbacher, Rev. Mod. Phys. **68**, 1125 (1996); C.S. Kim, T. Morozumi, A.I. Sanda, Phys. Rev. D **56**, 7240 (1997)
30. N.G. Deshpande, J. Trampetic, Phys. Rev. D **60**, 2583 (1988); A.J. Buras, M. Münz, Phys. Rev. D **52**, 186 (1995); A. Ali, G.F. Giudice, T. Mannel, Z. Phys. C **67**, 417 (1995)
31. Particle Data Group, C. Caso et al., Eur. Phys. J. C **3**, 1 (1998)
32. M. Misiak, Nucl. Phys. B **393**, 23 (1993); E: B **439**, 461 (1995); A.J. Buras, M. Münz, Phys. Rev. D **52**, (1995). Recently, the NNLO corrections in SM have been given: C. Bobeth, M. Misiak, J. Urban, Nucl. Phys. B **574**, 291 (2000); H.H. Asatryan, H.M. Asatrian, C. Greub, M. Walker, hep-ph/0109140
33. C.S. Huang, Commun. Theor. Phys. **2**, 1265 (1983)
34. R. Garisto, Phys. Rev. D **51**, 1107 (1995)
35. R. Garisto, G. Kane, Phys. Rev. D **44**, 2038 (1991)
36. D. Buskulic et al., ALEPH Collaboration, Phys. Lett. B **343**, 444 (1995); J. Kalinowski, Phys. Lett. B **245**, 201 (1990); A.K. Grant, Phys. Rev. D **51**, 207 (1995)
37. M. Ciuchini, G. Degrassi, P. Gambino, G.F. Giudice, Nucl. Phys. B **527**, 21 (1998) [hep-ph/9710335]; F.M. Borzumati, C. Greub, Phys. Rev. D **58**, 074004 (1998) [hep-ph/9802391]
38. C. Huang, T. Li, W. Liao, Q. Yan, S.H. Zhu, Eur. Phys. J. C **18**, 393 (2000) [hep-ph/9810412]
39. S. Bertolini et al., Phys. Rev. Lett. **59**, 180 (1987); N. Deshpande et al., ibid. **59**, 183 (1987); B. Grinstein et al., Phys. Lett. B **202**, 138 (1988); R. Grigjanis et al., ibid. **224**, 209 (1989); G. Cell et al., ibid. **248**, 181 (1990); B. Grinstein et al., Nucl. Phys. B **339**, 269 (1990)
40. A.J. Buras, hep-ph/9806471, and references therein
41. CLEO Collaboration, hep-ex/9908022; ALEPH Collabration, Phys. Lett. B **429**, 169 (1998)
42. Belle Progress Report, Belle Collaboration, KEK-PROGRESS-REPORT-97-1 (1997); Status of the BaBar Detector, BaBar Collaboration, SLAC-PUB-7951, presented at 29th International Conference on High Energy Physics, Vancouver, Canada, 1998